Dyes and Pigments 93 (2012) 1532–1537

Contents lists available at SciVerse ScienceDirect

Dyes and Pigments

journal homepage: www.elsevier.com/locate/dyepig

Review

Bright and stable Cy3-encapsulated fluorescent silica nanoparticles with a large Stokes shift

Gengwen Chen, Fengling Song*, Xu Wang, Shiguo Sun, Jiangli Fan, Xiaojun Peng*

State Key Laboratory of Fine Chemicals, Dalian University of Technology, No. 2 Linggong Road, High-tech District, Dalian 116024, PR China

ARTICLE INFO

Article history:
Received 5 July 2011
Received in revised form
2 September 2011
Accepted 5 September 2011
Available online 17 September 2011

Keywords:
Cyanine dyes
Fluorescence
HFRET
Silica nanoparticles
Stokes shift
Photostability

ABSTRACT

Traditional organic fluorophores, like cyanine dyes, suffer from their poor stability and weak brightness of individual molecule. In this work, a novel cyanine dye with a large Stokes shift (~75 nm) was encapsulated inside silica nanoparticles. The obtained small fluorescent silica nanoparticle (FSNP) exhibits more than ten times brightness than the free dye. The enhanced fluorescence brightness was assigned to the less homo Förster resonance energy transfer (HFRET) between multiple fluorophores, which was confirmed by the longer fluorescence lifetime of FSNP with a large Stokes shift than that with a normal Stokes shift. The FSNP's photostability is much better than organic fluorophores and comparable with that of Quantum Dots. When used in bioimaging, the FSNP remained a stable fluorescence signal, while the control free dye faded within 12 h.

1. Introduction

Bioanalysis and disease diagnosis call for highly bright fluorophores to assure the ultra sensitivity for trace targets [1,2]. Quantum Dots (QDs) have emerged to satisfy the requirement and have been explored as a hot research in the latest decade. However, it has been doubtful whether QDs could be widely used in bioanalysis applications due to their potential cytotoxicity, blinking and size-dependent fluorescence [3–6]. Traditional organic fluorophores, like cyanine dyes, suffer from their poor photostability, which limit their applications [7]. As an alternative, fluorescent silica nanoparticles (FSNPs) encapsulated organic fluorophores have attracted much attention in biotechnology and nanotechnology, [5,6,8] due to their better biocompatibility and less toxicity than QDs. At the same time, FSNPs were proved to have much better photostability than free organic fluorophores and comparable photostability with QDs [9]. Moreover, FSNPs can afford simple chemistry for surface modification and uniform nanoparticle size in different wavelength regions [10].

Even though FSNPs have many advantages, their sizes and fluorescence brightness have an annoying inverse proportion relationship [5]. While NPs' size was decreased to less than 50 nm, the fluorescence enhancement was found less than 20 times [11–15]. In many cases, the FSNP's fluorescence were quenched compared to the corresponding free dyes [16,17].

The potential quenching mechanism involves efficient nonradiative rates and fast energy transfer between the closely packed fluorophores within solid matrix. To address these problems, Wiesner et al. developed bright and stable FSNPs with a core-shell structure which can inhibit efficient nonradiative decay [12,13]. Nooney et al. correlated the fluorescence quenching with a fast homo Förster resonance energy transfer (HFRET) between multiple fluorophores inside nanoparticles [18,19]. It was suggested that an efficient way to inhibit the fast HFRET should be to employ fluorophores with a large Stokes shift [20].

Unfortunately most widely used organic fluorophores, like traditional cyanine dyes, have a small Stokes shift of 15–30 nm. Recently one new class of cyanine dyes with a large Stokes shift have been developed in our lab [21]. Here, we employ such a trimethine cyanine dye (Stokes shift 74 nm) to form a new FSNP with a core-shell structure, which shows more than ten times fluorescence brightness than its control free dye. At the same time, its photostability and biostability were found much better than those of the free control dyes.

* Corresponding authors. Tel.: +86 411 84986307; fax: +86 411 84986307.
E-mail addresses: songfl@dlut.edu.cn (F. Song), pengxj@dlut.edu.cn (X. Peng).

0143-7208/$ – see front matter © 2011 Elsevier Ltd. All rights reserved.
doi:10.1016/j.dyepig.2011.09.002

2. Experimental

2.1. Materials and methods

All the reactions were carried out under a nitrogen atmosphere with dry, freshly distilled solvents under anhydrous conditions, unless otherwise noted. Tetrahydrofuran (THF) was distilled from sodium-benzophenone, and methylene chloride (CH_2Cl_2) was distilled from calcium hydride. Silica gel (100–200 mesh) was used for flash column chromatography.

^{1}H-NMR and ^{13}C-NMR spectra were recorded on a VARIAN INOVA-400 spectrometer with chemical shifts reported as ppm (in $CDCl_3$, TMS as internal standard). Mass spectrometric data were obtained on a Q-TOF Micro mass spectrometry. Fluorescence measurements were performed on a PTI-700 Felix and Time-Master system, visible absorption spectra were determined using an HP-8453 spectrophotometer. Luminescence lifetimes were measured on a Horiba Jobin Yvon Fluoro Max-4 (TCSPC) instrument. The size and shape of silica nanoparticles were characterized by transmission electron microscope, TEM (JEM-1200EX). The following abbreviations are used to indicate the multiplicities: s, singlet; d, doublet; t, triplet; q, quartet; m, multiplet; br, broad.

2.2. Synthetic routes of the dyes

2.2.1. 1-ethyl-2,3,3-trimethyl-3H-indolenium iodide

A mixture of 2,3,3-trimethyl-3H-indole (31.8 g, 0.2 mol) and ethyl iodide (62.4 g) was refluxed in 300 mL toluene for 6 h. Upon being cooled to room temperature, the reaction mixture precipitated. The solid was filtered and washed with cold diethyl ether to give a pink power. Yield: 54 g; 86%.

2.2.2. 1-Ethyl-3,3-dimethyl-2-metheneindoline

1-ethyl-2,3,3-trimethyl-3H-indolenium iodide (12.6 g, 40 mmol) was dissolved in NaOH solution (100 mL, 20%). The mixture was stirred for 1 h at room temperature, and then extracted with ethyl ether (3 × 50 mL). The obtained organic layer was dried over anhydrous Na_2SO_4, evaporated under vacuum to give a light yellow oil (7 g, 94%), which was slowly changing into purple compound exposed to air.

2.2.3. 1,3-bis(1-ethyl-3,3-dimethylindolin-2-ylidene)propan-2-one (**1**)

1-Ethyl-3,3-dimethyl-2-metheneindoline (6.54 g, 35 mmol) and triethylamine (4.1 g, 40 mmol) were stirred in 30 mL anhydrous THF at 0 °C [22]. A solution of triphosgene (1.71 g, 17.5 mmol) dissolved in 10 mL dry THF was subsequently added dropwise at 0 °C. After the addition, the mixture was stirred at room temperature for 5 h. After the solvents were removed, the residue was purified by a column chromatography (SiO_2; methylene chloride/petroleum ether = 1:1) to afford a yellow powder product 1 (4.63 g, 67%). ^{1}H-NMR (400 MHz, $CDCl_3$): δ 1.15 (t, 6.8 Hz, 3H, CH_3), δ 1.71 (s, 6H, CH_3), δ 3.74 (q, 6.8 Hz, 2H, CH_2), δ 5.59 (s, 1H, CH), δ 6.84 (d, 8 Hz, 1H, Ar), δ 6.87 (t, 7.6 Hz, 1H, Ar), δ 7.15 (t, J = 7.6, 1H, Ar), δ 7.2 (d, 3.2 Hz, 1H, Ar). ^{13}C-NMR (100 MHz, $CDCl_3$): 10.82, 23.86, 36.26, 45.56, 104.69, 120.57, 121.46, 127.33, 137.63, 141.61, 165.20, 183.94. HRMS: m/z calcd $(M + H)^+$ for $C_{27}H_{33}N_2O^+$ 401.2587; found, 401.2981.

*2.2.3.1. Compound **2**.* A solution of compound **1** (4.0 g, 10 mmol) in THF (30 mL) was heated to reflux under nitrogen. $POCl_3$ (0.92 mL, 10 mmol) was added dropwise to the above solution under stirring when reflux. After addition, the mixture was refluxed for 2 h with the color change of the mixture from yellow to carmine. The solvent was evaporated under reduced pressure. The column chromatography (SiO_2; methylene chloride/methanol = 10:1) to afford a red powder (4 g, 95%).

^{1}H-NMR (400 MHz, $CDCl_3$): δ 1.37 (t, 7.2 Hz, 3H, CH_3), δ 1.519 (t, 7.2 Hz, 3H, CH_3), δ 1.64 (s, 6H, CH_3), δ 1.83 (s, 6H, CH_3), δ 4.08 (q, 7.2 Hz, 2H, CH_2), δ 4.38 (q, 7.2 Hz, 2H, CH_2), δ 5.78 (s, 1H, CH), δ 7.23 (d, 8.0 Hz, 1H, Ar), δ 7.27 (t, 8.0 Hz, 1H, Ar), δ 7.41 (t, 6.4 Hz, 1H, Ar), δ 7.48 (t, 7.6 Hz, 1H, Ar), δ 7.54 (d, 6.8 Hz, 1H, Ar), δ 7.58 (t, 8 Hz, 1H, Ar), δ 7.63(d, 8 Hz, 1H, Ar). ^{13}C-NMR (100 MHz, $CDCl_3$): 12.23, 13.71, 25.53, 25.99, 28.68, 39.47, 43.65, 44.75, 49.55, 53.34, 71.66, 96.08, 110.21, 113.26, 122.46, 123.20, 125.15, 127.83, 128.80, 129.66, 139.60, 139.72, 140.26, 140.52, 141.71, 164.63, 176.80. HRMS: m/z calcd M^+ for $C_{27}H_{31}N_2^+$ 383.2482; found, 383.2495.

*2.2.3.2. Compound **3a**.* To a solution of compound **2** (0.55 g, 1.31 mmol) in anhydrous THF (20 mL) was added APTES (0.1 mL) dropwise over 5 min at room temperature under a nitrogen atmosphere, the mixture was stirred at room temperature for 2 h. The color of the mixture changed from red to yellow. The solvents were evaporated under reduced pressure. A yellow powder product (0.36 g, 42.9%) was isolated by a column chromatography (SiO_2; methylene chloride/methanol = 100:6).

^{1}H-NMR (400 MHz, $CDCl_3$): δ 0.66 (t, 8 Hz, 2H, CH_2), δ 1.16 (t, 4 Hz, 12H, CH_3), δ 1.41 (t, 8 Hz, 3H, CH_3), δ 1.50 (s, 6H, CH_3), δ 1.61 (s, 6H, CH_3), δ 1.97 (m, 8 Hz, 2H, CH_2), δ 3.23–3.27 (b, 2H, CH_2), δ 3.76 (q, 7.2 Hz, 8H, CH_2), δ 4.11 (q, 6.4 Hz, 2H, CH_2), δ 5.16 (s, 1H, CH), δ 5.30 (s, 1H, CH), δ 6.82 (d, 8 Hz, 1H, Ar), δ 6.89 (d, 3.6 Hz, 1H, Ar), δ 7.06 (t, 7.2 Hz, 2H, Ar), δ 7.17 (d, 6.8 Hz, 1H, Ar), δ 7.23–7.29 (m, 1H, Ar); HRMS: m/z calcd M^+ for $C_{36}H_{54}N_3O_3Si$ 604.3934; found, 604.3920.

*2.2.3.3. Compound **3b**.* A mixture of 6-aminohexanoic acid (2.60 g, 20 mmol) and compound **2** (4.82 g, 11.5 mmol) were dissolved in anhydrous THF (40 mL) at room temperature under a nitrogen atmosphere. The purification procedure is similar to that of 3a. The desired product (2.97 g, 46%) was obtained by a column chromatography (SiO_2; methylene chloride/methanol = 100:6).

^{1}H-NMR (400 MHz, $CDCl_3$): δ 1.16 (m, 2H, CH2), δ 1.42 (t, 8 Hz, 3H, CH_3), δ 1.49 (s, 12H, CH_3), δ 1.73 (m, 4 Hz, 2H, CH_2), δ 1.91 (m, 2H,CH_2), δ 2.57 (t, 4 Hz, 2H, CH_2), δ 3.20 (s, 1H, NH), δ 3.78 (m, 2H, CH_2), δ 4.09 (q, 8 Hz, 2H, CH_2), δ 5.19 (s, 1H, CH), δ 6.86 (d, 8 Hz, 1H, ArH), δ 6.92 (d, 7.2 Hz, 1H, ArH), δ 7.06 (t, 7.2 Hz, 2H, ArH), δ 7.17 (d, 6.8 Hz, 1H, ArH), δ 7.23–7.29 (m, 3H, Ar); HRMS: m/z calcd M^+ for $C_{33}H_{44}N_3O_2$ 514.3428; found, 514.3433.

*2.2.3.4. Compound **3c**.* Compound **3c** was facilely synthesized in high yield by the procedure as published in the literature [23]. ^{1}H-NMR (400 MHz, $CDCl_3$): δ 1.49 (t, 7.2 Hz, 3H, CH_3), δ 1.63 (m, 6 Hz, 2H, CH_2), δ 1.72 (s, 12H, CH_3), δ 1.79 (m, 6.8 Hz, 2H, CH_2), δ 1.88 (m, 6.8 Hz, 2H, CH_2), δ 2.54 (t, 7.8 Hz, 2H, CH_2), δ 4.14 (t, 8 Hz, 2H, CH_2), δ 4.30 (q, 7.2 Hz, 2H, CH_2), δ 6.89 (d, 1.2 Hz, 1H, Ar), δ 7.13 (d, 1.2 Hz, 2H, Ar), δ 7.18 (t, 8 Hz, 2H, Ar), δ 7.26 (m, 2H, Ar), δ 7.39 (m, 4H, Ar), δ 8.41 (t, 13.6 Hz, 1H, CH); HRMS: m/z calcd M^+ for $C_{31}H_{39}N_2O_2$ 471.3012; found, 471.3029.

*2.2.3.5. Compound **3d**.* Dye **3c** was dissolved in dry DMF, then N, N′-dicyclohexyl carbodiimide (DCC) (5 equiv/carboxyl group) and NHS (N-hydroxysuccinimide, 10 equiv/carboxyl group) were added at room temperature under nitrogen. After 24 h, APTES (1 equiv/carboxyl group) was added. The mixture was left to stir at room temperature for 8 h. The solvents were evaporated under reduced pressure. The product was purified by flash chromatography (SiO_2; methylene chloride/methanol = 100:4). The product was certified by mass spectrometry with the molecular peak of the fluorophore-conjugated APTES (m/z = 674.4349).

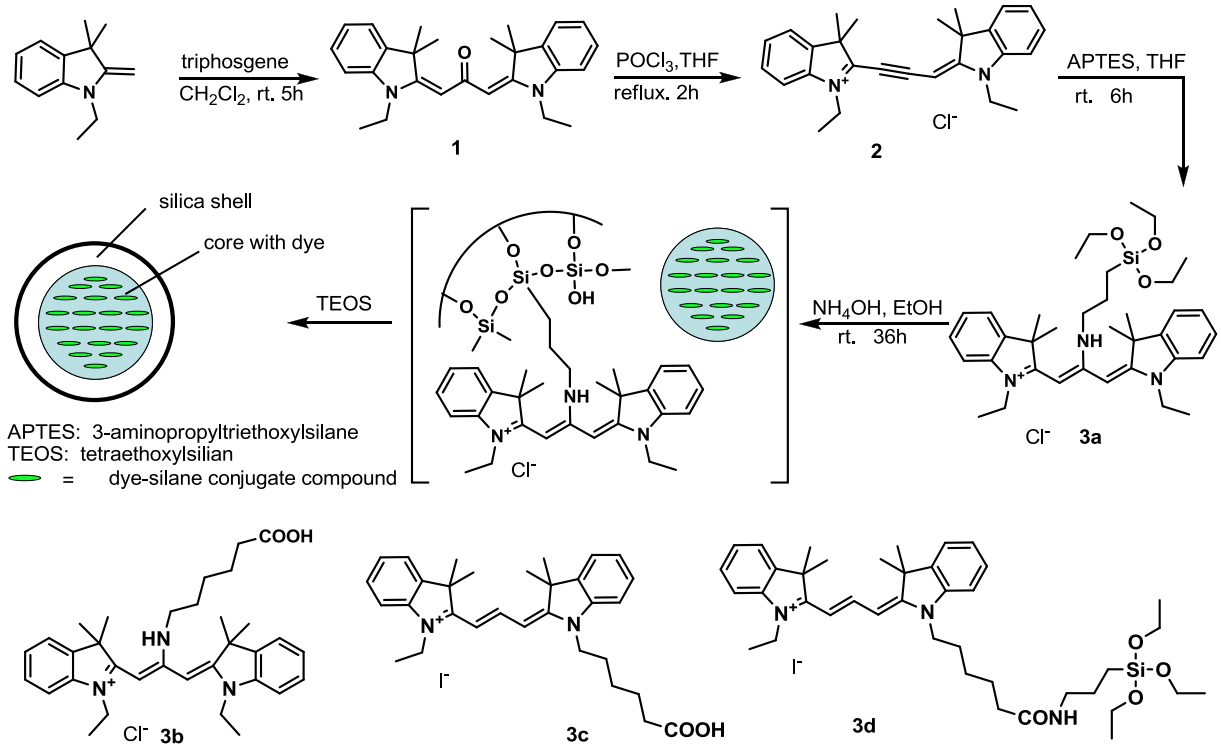

Scheme 1. Synthetic routes of the dyes.

2.3. UV–Vis absorption and photoluminescence spectroscopy

Fluorescence measurements were performed on a PTI-700 Felix and Time-Master system, visible absorption spectra were determined using an HP-8453 spectrophotometer. To quantify the brightness of the particles in comparison to free dye, standard absorption matching between free dye and particle solution by spectrophotometry and subsequent emission investigation of these matched solutions by spectrofluorometry was performed [20]. Free dyes, QD and fluorescence nanoparticles were dissolved in ethanol, with almost the same UV absorbance by adjusting concentration. The total amount of the Cy3 dye per unit volume can be derived through the absorption [24], we suppose that the amount of the Cy3 dye molecules in solution and FSNPs suspension are almost the same when they have equivalent UV absorbance value. Fluorescence spectra were obtained immediately, the excitation wavelengths of dye **3b**, dye **3c**, QD, **FSNP-A** and **FSNP-C** were 464 nm, 550 nm, 464 nm, 464 nm and 550 nm respectively. The fluorescence enhancement was evaluated by the fluorescence intensity at the maximum of the highest peak.

2.4. General method of synthesizing fluorescent silica nanoparticles

3a or **3d** was dissolved in 20 mL dried ethanol, then 1 mL ammonia and 40 μL deionized water were added with stirring. Core formed after 9 h of stirring, a shell of pure tetraethyl orthosilicate (TEOS) was added by controlled addition of 200 μL at a rate of 2 μL per minute. (Note: a stepwise addition of TEOS is necessary to keep the total amount of TEOS and hydrolyzed TEOS in the system at any time below the critical nucleation concentration to preserve non-fluorescent particles from forming.) After 12 h of stirring, nanoparticles were isolated by centrifugation at the speed of 14,000 rpm, and the isolated products were re-dispersion in ethanol. After repeating 3 times of washing and re-dispersion, the solution was centrifuged at the speed of 2000 rpm to remove any aggregated particles.

2.5. Determination of dye content of FSNPs

The yield of dye was determined quantitatively by UV–Vis spectroscopy. The presence of unencapsulated dye was determined by centrifuging. The concentration of dye in the supernatant was determined spectrophotometrically [17].

As the TEM characterization showed that the Cy3 doped core-shell FSNPs were uniform in size. The average volume per FSNPs was obtained from the TEM, see Eq. (1).

$$V = 4/3\pi(d/2)^3 \quad (1)$$

Where V is the average volume and d is the diameter determined by TEM. The converted amount of TEOS and the density of the FSNPs (corresponding to that of amorphous silica, ca. 2.2 g/cm^3), allowed

Table 1
Photophysical characteristics of dyes in ethanol at 1×10^{-5} M Molar extinction coefficients are in cm^{-1} M^{-1} and at the maximum of the highest peak.

Dye	λ_{ex} (nm)	λ_{em} (nm)	Stokes shift (nm)	ε ($\times 10^5$)	Φ_f
2	524	564	40	1.18	0.0027
3a	466	540	74	-[a]	0.0065
3b	464	536	72	0.54	0.0074
3c	550	571	21	0.94	0.095
FSNP-A	465	535	70		0.049[b]
FSNP-B	567	577	10		0.018[c]

The fluorescence quantum yields are measured relative to free Rhodamine B ($\Phi_f = 0.69$ in methanol).
[a] Free dye **3a** is not stable in ethanol.
[b] NPs which contain 392 molecules per FSNPs was measured.
[c] NPs which contain 138 molecules per FSNPs was measured.

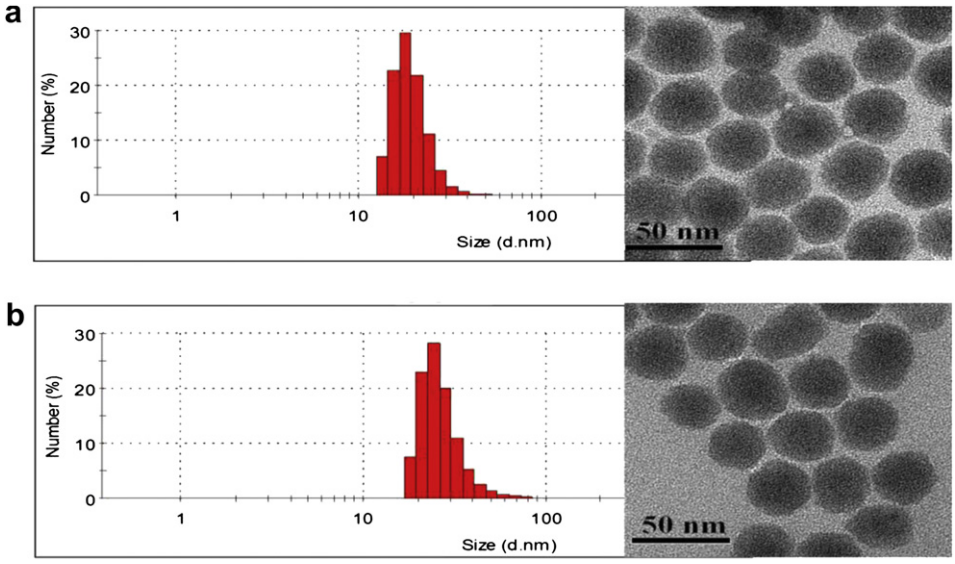

Fig. 1. The diameter distribution curves for **FSNP-A** (a) and **FSNP-C** (b) from DLS measurement (mean number percent) performed on an aqueous suspension of NPs (1.0 mg/mL). TEM images show FSNP's shape and size.

the estimation of the number of FSNPs in the suspension obtained at the end of the synthesis. As we know the total number of the Cy3 dye molecules in the suspension, the number of the Cy3 dye per FSNPs obtained from Eq. (2).

$$Np = Ncy3/Nnp \quad (2)$$

Where Np is the the number of the Cy3 dye per FSNPs, Ncy3 is the total number of the Cy3 dye molecules in the suspension and Nnp is the number of FSNPs in the suspension.

2.6. Photostability test

Free dyes, QD and fluorescence nanoparticles were dissolved in 3 mL H_2O, with almost the same UV absorbance by adjusting concentration. Samples were exposed to light under a W-Halogen lamp (200 W), the distance between lamp and samples is 30 cm. Absorption spectra of samples were taken after every 1 h.

2.7. Preparation and staining of cell cultures

MCF-7 cells were maintained in minimum essential medium (DMEM) supplemented with 10% fetal bovine serum, 100 units/mL penicillin and 100 μg/mL streptomycin. The cells were incubated at 37 °C in 5% CO_2. Two days before imaging, cells were plated on tissue culture plates. Cells were then incubated in fresh media at 37 °C, 5% CO_2. One day prior to imaging, the media was exchanged for 500 μL fresh media with FSNPs encapsulated **3a** (50 μg/mL) and free dye **3b** (5 μM) and the cells were incubated for 12 h. Luminescence imaging was performed after washing the cells three times with PBS buffer. After imaging, the cells were incubated at 37 °C in the presence fresh media for another 12 h. The cells were washed with PBS buffer for three times before imaging.

2.8. Fluorescence imaging experiments

Fluorescence imaging studies were performed with a Nikon eclipase TE2000-5 inverted fluorescence microscopy. The cells

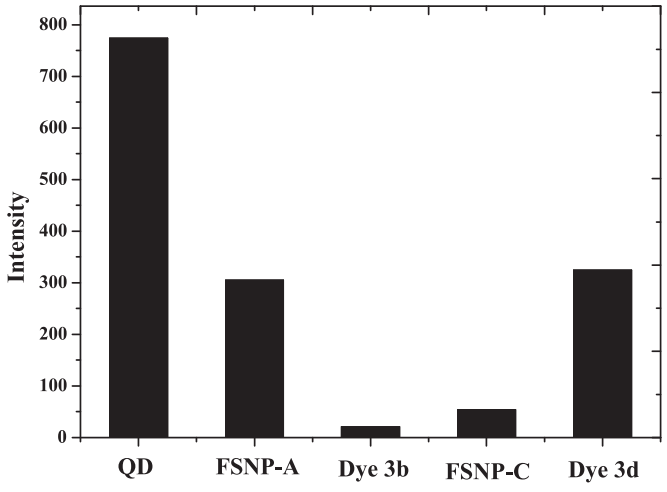

Fig. 2. Fluorescent intensity comparison of QD545, **FSNP-A** (392 molecules per nanoparticle), free dye **3b**, **3d** and **FSNP-C** (138 molecules per nanoparticle) in ethanol absolute. All samples were dispersed or dissolved in ethanol to a final concentration with almost the same absorbance (0.01).

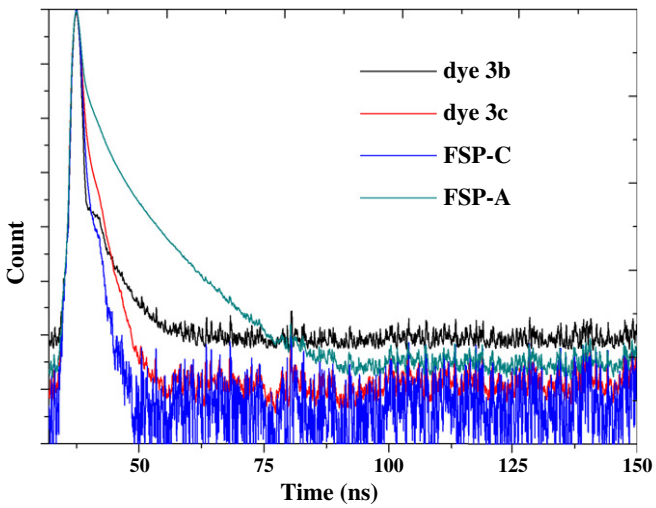

Fig. 3. Fluorescence decay of FSNPs and the control dyes. The concentration of free dyes is 5×10^{-5} M in ethanol, and the concentrations of FSNPs were adjusted to have the same absorbance with its corresponding free dye.

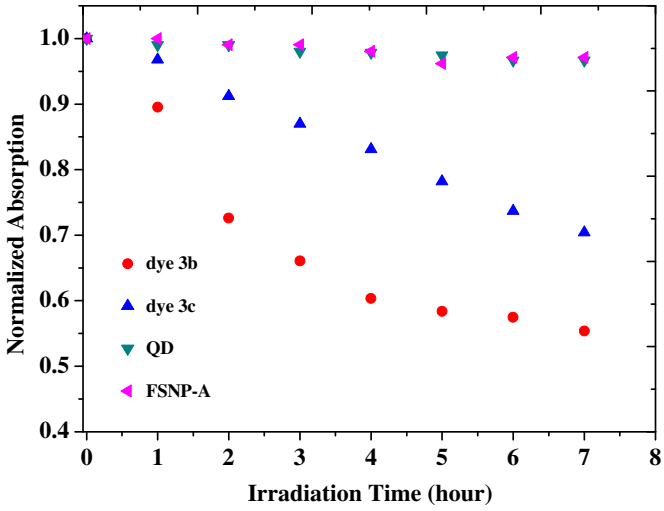

Fig. 4. Photostability evaluation of FSNPs and the control dyes under a W-Halogen lamp (200 W). Free dyes, FSNPs and QD were dissolved in deionized water, with almost the same UV absorbance by adjusting concentration. Values were represented for sequential measurements every 1 h.

were excited with green light and emission was collected by a 605–680 nm band pass filter. The microscope settings (brightness, contrast, and exposure time) were held constant before and after pretreatment of cells with FSNPs to compare the relative intensity of fluorescence. Image analysis was performed in Adobe Photoshop.

3. Results and disscusion

The fluorophores used for FSNPs were synthesized in our lab (Scheme 1). Compound **1** was obtained by condensation of *N*-Ethyl 3H indoline and triphosgene, following chlorination with phosphoryl chloride to give trimethine cyanine dye **2**. Dye **2** can transfer into its silicon ethoxide **3a** by an SNAr reaction [21]. One control dye **3b** was synthesized by similar procedure. Both free dyes **3a** and **3b** have a large Stokes shift (Table 1 and Fig. S1). For comparison, one cyanine dye **3c** with a small stokes shift and its silicon ethoxide **3d** was synthesized by previous reported methods [23]. Two FSNPs doped with **3a** and **3c** were synthesized by a modified Stöber protocol [13,16,20,25,26] (named as **FSNP-A** and **FSNP-C**). Both FSNPs possess the same core-shell structure to inhibit nonradiative decay [12].

The FSNPs sizes were characterized by dynamic light scattering (DLS) and TEM. It is shown **FSNP-A** has a particle diameter about 30–15 nm in the TEM photography. (Fig. 1) The **FSNP-A** made in optimized conditions is estimated to encapsulate about 392 dye molecules in one nanoparticle (Fig. 2 and Table S1). And its fluorescence quantum yield was 7.5 times of that of its free dye **3a** (Table 1). As shown in Fig. 2, the **FSNP-A** is about 14 times more fluorescent than its free control dye **3b** when the absorbance at λ_{max} of both solutions of **FSNP-A** and **3b** were adjusted to 0.01. Noteworthly, **FSNP-A** shows a comparable brightness with dye **3d**, even though weaker than a commercial QD (λ_{em} = 545 nm). In contrast, **FSNP-C** has much weaker fluorescence than the free dye **3c**, its fluorescence quantum yields of **FSNP-C** drop continuously when encapsulating dye molecules number from 13 to 1300 (Tables S1 and S2, and Fig. 2 and Figs. S7 and S8).

We attribute the difference of fluorescence properties between the two FSNPs to the different Stokes shift of their original dyes. The new dye **3a** with a large Stokes shift makes less efficient HFRET occur between dye molecules inside a nanoparticle, which leads to brighter fluorescence of **FSNP-A**. Fluorescence decay measurements were employed to confirm the less efficient HFRET in **FSNP-A** than in **FSNP-C**. The HFRET interaction happens between close pairs of dye molecules (excited one and unexcited one). It is a very fast process which can shorten fluorescence decay time [27,28]. As shown in Fig. 3, **FSNP-A** has much longer fluorescence decay than **FSNP-C** and the two free control dyes. This means that less efficient HFRET occurs in **FSNP-A** than in **FSNP-C**. From the above results, it

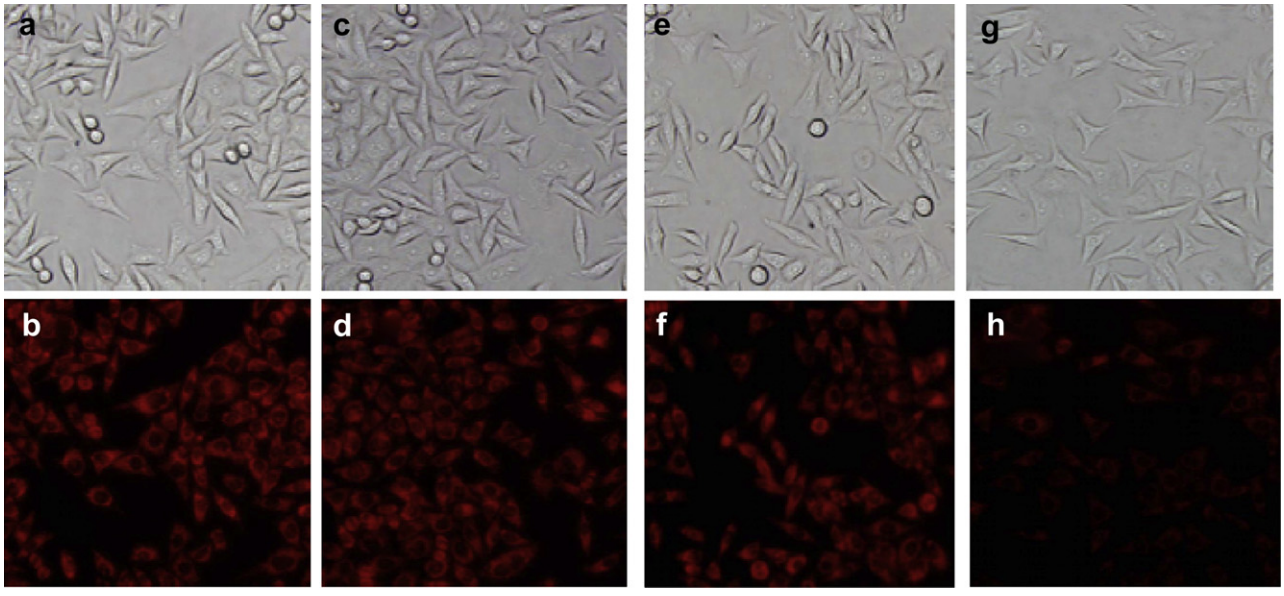

Fig. 5. Optical (up) and fluorescence (below) images of MCF-7 cells incubated with **FSNP-A** (50 μg/mL) (Fig. 5a–d) and dye 3b (5 μM) (Fig. 5e–h) in medium. Following uptake for 12 h at 37 °C, remaining free dyes and surface-bound FSNPs were washed by fresh medium. Images 5a, 5b, 5e and 5f were obtained immediately after washing under a Nikon eclipase TE2000-5 inverted fluorescence microscopy. The cells were excited with green light and emission was collected by a 605–680 nm band pass filter. After imaging, samples 5a, 5b, 5e and 5f were incubated with fresh media at 37 °C for another 12 h. Images 5c, 5d (labeled FSNP-A) and 5g, 5h (labeled with dye 3b) were obtained from confocal laser microscopy after incubating. The microscope settings (brightness, contrast and expose times (1/10.0 s)) were stayed the same during fluorescence imaging studies. (For interpretation of the references to colour in this figure legend, the reader is referred to the web version of this article.)

can be concluded that the large Stokes shift leads to brighter fluorescence. Although dye **3b** also has a large Stokes shift, it possesses a shorter decay time than **FSNP-A**. That may be due to its strong trend to form aggregation in solution which can quickly quench the fluorescence.

Conventional organic fluorophores usually suffer from their poor photostabilities, which limits their imaging time. A long tracking time is desirable for bioanalysis and disease diagnosis. The photostability of **FSNP-A** was compared with that of QD545 and the other two free dyes (dye **3b** and dye **3c**). As shown in Fig. 4, the **FSNP-A** shows comparable photostability with QD545, and much more stable than free organic fluorophores. This result is consistent with the other reports, [9,29] and ensures this new FSNP to have a longer imaging time than organic dyes. Besides the photostability, the stability of FSNPs in real biology environment is another key factor in practical applications. As shown in Fig. 5, **FSNP-A** was found to have better biostability than its free dye **3b** in the MCF-7 cells imaging experiments. After 12 h incubation with the fluorophores, both **FSNP-A** and **3b** stained cells were washed with PBS (Dulbecco's Phosphate Buffered Saline) buffer. A series of samples (**FSNP-A** (Fig. 5a and b), **3b** (Fig. 5e and f)) were imaged immediately. The other series of samples (**FSNP-A** (Fig. 5c and d), **3b** (Fig. 5g and h)) were imaged after being incubated with fresh media (37 °C, 5% CO_2) for another 12 h. We cannot find visible signal intensity of **FSNP-A** stained cells decreases by comparing Fig. 5b and f. But obvious signal intensity drops for **3b** stained cells by comparing Fig. 5d and h.

4. Conclusion

we successfully developed a novel FSNP encapsulated a cyanine dye with a large Stokes shift which leads to brighter fluorescence. And its excellent photostability and biostability were demonstrated by comparing with its control organic dyes. Due to its large Stokes shift, this new FSNP has potential to be used in imaging multiple biological events simultaneously [30]. Current efforts in our lab are to develop near-infrared FSNPs with a large Stokes shift and to apply these FSNPs into bioanalysis.

Acknowledgments

This work was supported financially by the NSF of China (20706008, 20705621, 20876024, 20923006 and 21006009), National Basic Research Program of China (2009CB724700), the Fundamental Research Funds for the Central Universities, Ministry of Education of China (Program for Changjiang Scholars and Innovative Research Team in University, IRT0711; and Cultivation Fund of the Key Scientific and Technical Innovation Project, 707016), Science Program (2010J21DW001) of Dalian City, and Innovative Research Team of Liaoning Provincec (2006T026).

Appendix. Supporting information

Supplementary data related to this article can be found online at doi:10.1016/j.dyepig.2011.09.002.

References

[1] Sutedja TG, Venmans BJ, Smit EF, Postmus PE. Fluorescence bronchoscopy for early detection of lung cancer – a clinical perspective. Lung Cancer-J Iaslc 2001;34(2):157–68.
[2] Chen X, Zhou Y, Peng X, Yoon J. Fluorescent and colorimetric probes for detection of thiols. Chem Soc Rev 2010;39(6):2120.
[3] Gould P. Criteria set for quantum dot clinical safety. Nano Today 2007;2(6):9.
[4] Choi HS, Liu W, Misra P, Tanaka E, Zimmer JP, Ipe BI, et al. Renal clearance of quantum dots. Nat Biotechnol 2007;25(10):1165–70.
[5] Wang L, Zhao WJ, Tan WH. Bioconjugated silica nanoparticles: development and applications. Nano Res 2008;1(2):99–115.
[6] Jeon YH, Kim YH, Choi K, Piao JY, Quan B, Lee YS, et al. In vivo imaging of sentinel nodes using fluorescent silica nanoparticles in living mice. Mol Imaging Biol 2010;12(2):155–62.
[7] Lavis LD, Raines RT. Bright ideas for chemical biology. Acs Chem Biol 2008; 3(3):142–55.
[8] Seo S, Lee HY, Park M, Lim JM, Kang D, Yoon J, et al. Fluorescein-functionalized silica nanoparticles as a selective fluorogenic chemosensor for Cu^{2+} in living cells. Eur J Inorg Chem 2010;2010(6):843–7.
[9] Nakamura M, Shono M, Ishimura K. Synthesis, characterization, and biological applications of multifluorescent silica nanoparticles. Anal Chem 2007;79(17): 6507–14.
[10] Knopp D, Tang DP, Niessner R. Bioanalytical applications of biomolecule-functionalized nanometer-sized doped silica particles. Anal Chim Acta 2009; 647(1):14–30.
[11] Tian Z, Shaller AD, Li ADQ. Twisted perylene dyes enable highly fluorescent and photostable nanoparticles. Chem Commun 2009;(2):180–2.
[12] Larson DR, Ow H, Vishwasrao HD, Heikal AA, Wiesner U, Webb WW. Silica nanoparticle architecture determines radiative properties of encapsulated fluorophores. Chem Mater 2008;20(8):2677–84.
[13] Ow H, Larson DR, Srivastava M, Baird BA, Webb WW, Wiesner U. Bright and stable core-shell fluorescent silica nanoparticles. Nano Lett 2005;5(1): 113–7.
[14] Alberto G, Miletto I, Viscardi G, Caputo G, Latterini L, Coluccia S, et al. Hybrid cyanine-silica nanoparticles: homogeneous photoemission behavior of entrapped fluorophores and consequent high brightness enhancement. J Phys Chem C 2009;113(50):21048–53.
[15] Miletto I, Gilardino A, Zamburlin P, Dalmazzo S, Lovisolo D, Caputo G, et al. Highly bright and photostable cyanine dye-doped silica nanoparticles for optical imaging: photophysical characterization and cell tests. Dyes Pigments 2010;84(1):121–7.
[16] Ha SW, Camalier CE, Beck GR, Lee JK. New method to prepare very stable and biocompatible fluorescent silica nanoparticles. Chem Commun 2009;(20):2881–3.
[17] Bringley JF, Penner TL, Wang RZ, Harder JF, Harrison WJ, Buonemani L. Silica nanoparticles encapsulating near-infrared emissive cyanine dyes. J Colloid Interf Sci 2008;320(1):132–9.
[18] McDonagh C, Stranik O, Nooney R, MacCraith BD. Nanoparticle strategies for enhancing the sensitivity of fluorescence-based biochips. Nanomedicine-UK 2009;4(6):645–56.
[19] Nooney RI, McCahey CMN, Stranik O, Guevel XL, McDonagh C, MacCraith BD. Experimental and theoretical studies of the optimization of fluorescence from near-infrared dye-doped silica nanoparticles. Anal Bioanal Chem 2009;393(4): 1143–9.
[20] Herz E, Burns A, Bonner D, Wiesner U. Large stokes-shift fluorescent silica nanoparticles with enhanced emission over free dye for single excitation multiplexing. Macromol Rapid Comm 2009;30(22):1907–10.
[21] Peng XJ, Song FL, Lu E, Wang YN, Zhou W, Fan JL, et al. Heptamethine cyanine dyes with a large stokes shift and strong fluorescence: a paradigm for excited-state intramolecular charge transfer. J Am Chem Soc 2005; 127(12):4170–1.
[22] Zhang D, Su JH, Ma X, Tian H. An efficient multiple-mode molecular logic system for pH, solvent polarity, and Hg^{2+} ions. Tetrahedron 2008;64(36): 8515–21.
[23] Jung ME, Kim WJ. Practical syntheses of dyes for difference gel electrophoresis. Bioorgan Med Chem 2006;14(1):92–7.
[24] He XX, Chen JY, Wang KM, Qin DL, Tan WH. Preparation of luminescent Cy5 doped core-shell SFNPs and its application as a near-infrared fluorescent marker. Talanta 2007;72(4):1519–26.
[25] Montalti M, Prodi L, Zaccheroni N, Zattoni A, Reschiglian P, Falini G. Energy transfer in fluorescent silica nanoparticles. Langmuir 2004;20(7): 2989–91.
[26] Vanblaaderen A, Vrij A. Synthesis and characterization of colloidal dispersions of fluorescent, monodisperse silica spheres. Langmuir 1992;8(12): 2921–31.
[27] Imhof A, Megens M, Engelberts JJ, de Lang DTN, Sprik R, Vos WL. Spectroscopy of fluorescein (FITC) dyed colloidal silica spheres. J Phys Chem B 1999;103(9): 1408–15.
[28] Viger ML, Live LS, Therrien OD, Boudreau D. Reduction of self-quenching in fluorescent silica-coated silver nanoparticles. Plasmonics 2008;3(1):33–40.
[29] Lian W, Litherland SA, Badrane H, Tan WH, Wu DH, Baker HV, et al. Ultrasensitive detection of biomolecules with fluorescent dye-doped nanoparticles. Anal Biochem 2004;334(1):135–44.
[30] Pham W, Cassell L, Gillman A, Koktysh D, Gore JC. A near-infrared dye for multichannel imaging. Chem Commun 2008;(16):1895–7.